COMPDYN 2015
5th ECCOMAS Thematic Conference on
Computational Methods in Structural Dynamics and Earthquake Engineering
M. Papadrakakis, V. Papadopoulos, V. Plevris (eds.)
Crete Island, Greece, 25–27 May 2015

SEISMIC PROTECTION OF HEAVY NON-STRUCTURAL MONOLITHIC OBJECTS AT THE TOP OF A HISTORICAL MASONRY CONSTRUCTION THROUGH BASE ISOLATION

A. Chiozzi[1], M. Simoni[1], and A. Tralli[1]

[1] University of Ferrara
Department of Engineering
I44122 – 1, Via Saragat – Ferrara (ITALY)
e-mail: {andrea.chiozzi, michele.simoni, tra}@unife.it

Keywords: Seismic Protection, Non-structural objects, Base Isolation, Masonry.

Abstract. *This contribution addresses the problem of earthquake protection of heavy non-structural monolithic objects, which are usually placed at the top of historical masonry constructions for mainly decorative purposes like pinnacles, merlons, sculptures and heavy artwork. Such objects, when subjected to base accelerations due to seismic actions, may undergo rocking phenomena, which may eventually lead to the overturning of the whole body. In particular, the specific case of the seismic protection of ancient marble pinnacles placed at the top of a three-arched masonry city gate in Ferrara (ITALY) is illustrated. In a preliminary rocking analysis, the pinnacles have been idealized as rigid bodies in unilateral contact with the underlying moving base and the resulting rocking motion have been analyzed. The structural safety level of the pinnacles have thus been assessed. As a consequence of these considerations, a base isolation system designed around multiple double concave curved-surface steel sliders have been devised. The effectiveness of the proposed isolation system has been assessed through numerical simulations. The amplification effect of the ground acceleration due to the underlying three-arched structure has been established through time-history dynamic analyses, where masonry has been considered as a viscoelastic material. To this aim, an equivalent viscous damping coefficient has been calculated for masonry following an iterative procedure involving the computation of capacity curves for both in- and out-of-plane load directions and the definition of simplified bi- and tri-linear inelastic load-displacement capacity curves for masonry panels.*

1 INTRODUCTION

Many research efforts have been devoted, in the past, to the prevention of seismic damage of civil and industrial constructions, both modern and historical. Among the many aspects that are targeted in these studies, an increasing attention is being addressed towards the understanding of the seismic behavior of non-structural elements belonging to such constructions. The ultimate goal is to devise effective seismic protection systems for heavy artwork, sculptures, pinnacles, and similar objects which do not have a structural function but belong to world heritage and, in many cases, have an inestimable value; for an introduction to this subject the reader is addressed to [1], [2], [3], [4], [5], [6], [7].

The aim of the present contribution is to illustrate the case study of the seismic protection through base isolation of eleven ancient marble pinnacles placed at the top of the three-arched masonry city gate in Ferrara, Italy, portrayed in Fig.1a, which underwent the 2012 Emilia seismic swarm.

(a) (b)

Figure 1: (a) Three-arched masonry city gate, Corso Giovecca, Ferrara, Italy; (b) damages from overturning of monolithic decorative elements during 2012 Emilia earthquake (Corso Giovecca, Ferrara, Italy).

From a mechanical point of view, in many cases, non-structural objects belonging to constructions are monolithic and therefore, they may be regarded as rigid bodies. The main phenomenon a rigid body undergoes when subject to earthquake excitations is an oscillating motion around different instantaneous rotation centers belonging to its base known as *rocking*, which may eventually lead to collapse due to the final toppling of the whole body.

In the study of pure rocking, a number of investigations have adopted a simple two-dimensional model, which was first proposed in [8], later derived independently in a seminal paper by Housner [9] and revised in [10]. The model is based on the assumption of no bouncing and sufficient friction to prevent sliding during impact.

Recently, new interest has been devoted to the study of seismic protection of the artistic heritage and several authors addressed the problem of the rocking motion of rigid bodies provided with base isolation systems ([12], [13], [14]) where the effectiveness of base isolation in increasing the safety level of art objects in case of earthquake has been assessed.

Finally, some three-dimensional models describing the dynamics of rigid bodies with impacts has been proposed in literature. In particular, the difficult problem of the three-dimensional motion of a an axisymmetric body rocking and rolling on a planar surface was addressed by [15], [16], [17].

The development of effective techniques for seismic risk mitigation of monolithic non-structural elements is a fundamental issue. A first approach [18] consists in anchoring objects

using different support mounts that essentially makes the object itself part of the structure. However, such a solution is not satisfying for it allows the transmission of large impulsive seismic forces which the object, being too brittle, cannot withstand. Furthermore, in this case the effects of the earthquake are usually not reversible.

An alternative approach consists in adopting base isolation systems which has been demonstrated to be an excellent solution in limiting the transferred seismic actions thus effectively mitigating the seismic risk on different types of structures [19]. Nevertheless, while base isolation for bridges or buildings has been largely developed in the last decades, base isolation for the comparatively much lighter art-objects and other kind of non-structural elements has not experienced the same level of development and it is still an open topic. As clearly pointed out in [20], even though the basic concepts which stand at the basis of base isolation systems are the same, the application of isolation techniques developed for civil structures to small objects requires more than a simple extension, and specific considerations are mandatory since the parameters governing the behavior of the seismic isolators need to be specifically calibrated.

As initially stated, the present paper addresses the problem of the structural safety assessment and seismic protection of heavy monolithic objects placed at the top of a monumental construction through the illustration of a specific case study which concerns the seismic risk mitigation for eleven marble pinnacles placed at the top of a three-arched masonry city gate built in Ferrara (Fig.1a), Italy, at the end of Corso della Giovecca, between 1703 and 1704 a.C. The marble pinnacles placed at the top of the gate have mainly a decorative purpose and their slenderness, coupled with their considerable mass, makes them highly vulnerable to seismic actions so that they cannot be considered safe. After the strong seismic events which struck Emilia in May 2012 and caused severe damage to the city's historical constructions, the pinnacles have been removed for safety reasons. In Fig.1b damages produced by a monolithic decorative non-structural element collapsed in Ferrara during 2012 Emilia earthquake is shown.

In order to protect the pinnacles from seismic actions, a specific base isolation system, based on the use of multiple double concave curved surface steel sliders. The proposed application, at the best of the authors' knowledge, is very peculiar and it is the first example in Italy of base isolation of heavy marble pinnacles at the top of a monumental construction.

The paper is organized as follows. In Section 2 the underlying three-arched masonry city gate structure is characterized from a dynamical point of view, a natural frequency analysis have been conducted and capacity curves for the masonry structure have been computed. In Section 3 the rocking behavior of the single pinnacle subject to ground accelerations is assessed. In Section 4 the proposed base isolation systems is described and in Section 5 its effectiveness is established through numerical simulations, which involves the evaluation of the amplification effect of the underlying masonry structure and the definition of equivalent viscous damping coefficients. In Section 6 conclusions and future research direction are given.

2 THE FERRARA MASONRY CITY GATE

The case study considered in the present work is a three-arched masonry construction whose geometry is shown in Fig.2a. The structure is in good general conditions and is made of clay artificial bricks and mortar. Eleven decorative marble pinnacles stand at the top of the gate.

Each pinnacle, whose geometry is portrayed in Fig.2b, is made of different axisymmetric marble blocks piled and bonded together by a central iron rod. A pinnacle may be regarded as an axisymmetric rigid body, which may undergo rocking motion when subjected to base excitations. As shown in Fig.2b, the pinnacle is 2.37 m tall and its circular base has a diameter B

of 0.60 m. Marble is assumed to have a density ρ of 2700 kg/m^3 and the resulting mass M of the pinnacle is 980 kg. Pinnacles are placed on two different orders; more precisely eight pinnacles are placed at an intermediate height of 9.80 m (hereinafter referred to as *lateral pinnacles*) and three pinnacles are placed on the top of the gate at a height of 18.50m (hereinafter referred to as *central pinnacles*).

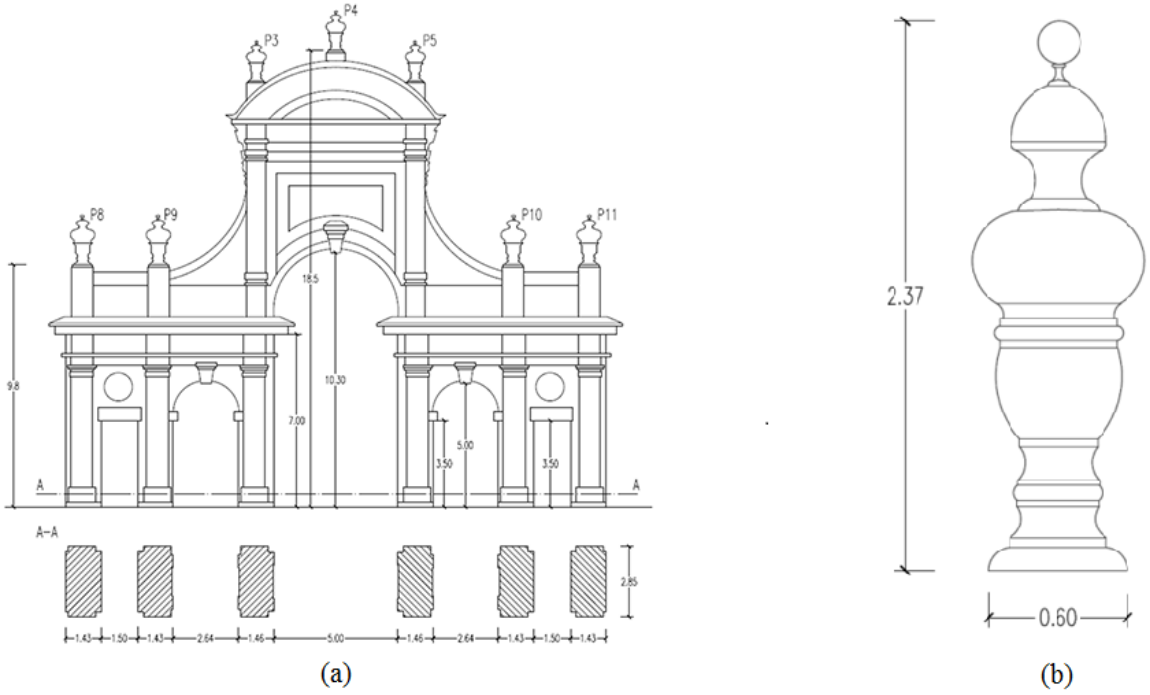

Figure 2: (a) Geometric representation of the three-arched masonry city gate; (b) Geometric representation of the pinnacle.

2.1 The design seismic action

Given the WGS84 coordinates for the city-gate location (44.832 N, 11.632 E), assuming a return period for the design seismic event of 712 years (i.e. corresponding to the ultimate limit

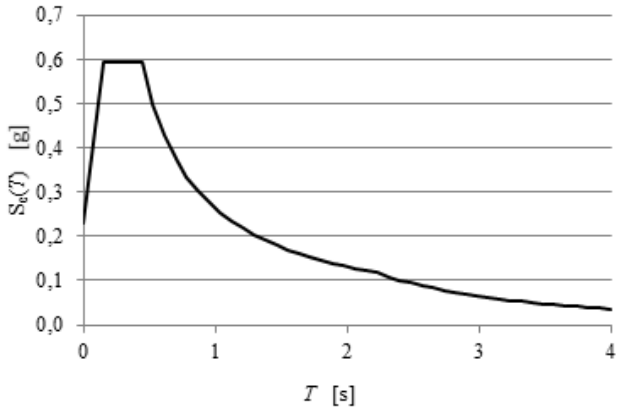

Figure 3: Design earthquake spectra for the three-arched masonry city gate according to NTC2008.

state in terms of life safety for a Class III structure and soil category C, in agreement with the Italian Building Code [20] the resulting design seismic action on the construction is determined. The corresponding design earthquake spectra is reported in Fig.3.

2.2 Natural frequency analysis of the masonry structure

In order to evaluate the fundamental period T_1 of the three-arched masonry structure and to establish its main vibration modes a linear finite element natural frequency analysis has been carried out using the finite element analysis software Straus7 [21]. The FEM model has been discretized with eight node brick-type finite elements and is shown in Fig.4a. The mechanical properties of the masonry material are reported in Tab.1 and are determined according to prescriptions contained in [22] for existing constructions.

Compressive strength f_m [MPa]	Shear strength τ_0 [MPa]	Elastic modulus E [MPa]	Tangential modulus G [MPa]	Specific weight w [kN/m^3]
2.4	6.0	1200	400	18

Table 1 Material parameters for masonry.

Mode	Frequency [Hz]	Participating mass in the in-plane direction [%]	Participating mass in the out-of-plane direction [%]
1	2.0131	0.00	54.54
2	6.0679	0.01	0.00
3	6.4394	87.96	0.00
4	7.5946	0.00	26.44

Table 2 Frequency and participating mass for the four vibration modes.

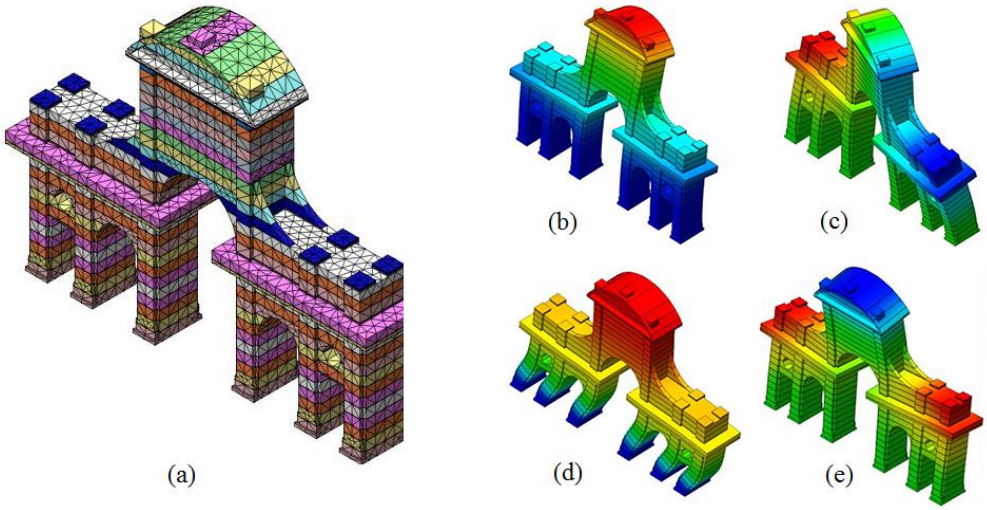

Figure 4: (a) Finite element model of the three-arched masonry city gate for natural frequency analysis; the first four vibration modes: (b) translational mode in the out-of-plane direction, (c) torsional mode, (d) translational mode in the in-plane direction, (e) partial translational model in the out-of-plane direction.

From the analysis, three pure translational and a torsional mode have been obtained as the main four vibration modes which are represented in Fig.4b. Tab.2 contains frequency and participating mass in the in-plane and out-of-plane directions for the four modes.

2.3 In- and out-of-plane capacity curves for the masonry structure

Using the commercial finite-element analysis software DIANA [23], in- and out-of-plane capacity curves for the masonry structure have been determined. The finite element model used is shown Fig. 4a. The masonry material has been assigned a *total strain crack model* constitutive law [23]. As shown in the previous paragraph the principal vibration mode in the in-plane direction is the third mode with a participating mass of 87.6%. Thus, a distribution of forces proportional to the third mode has been applied and the capacity curve have been computed through a finite-element non-linear incremental analysis. The same analysis has been conducted for the out-of-plane direction with a distribution of forces proportional to the first vibration mode, which is the principal mode in the out-of-plane direction with a participating mass of 54.54. The obtained in- and out-of-plane capacity curves, shown in Fig. 5, relates the total shear force F_b applied at the base of the structure with the in- and out-of-plane displacements d_c of a control point, which has been chosen as the medial point placed on one of the short sides of the construction, at a height of 3.00 m.

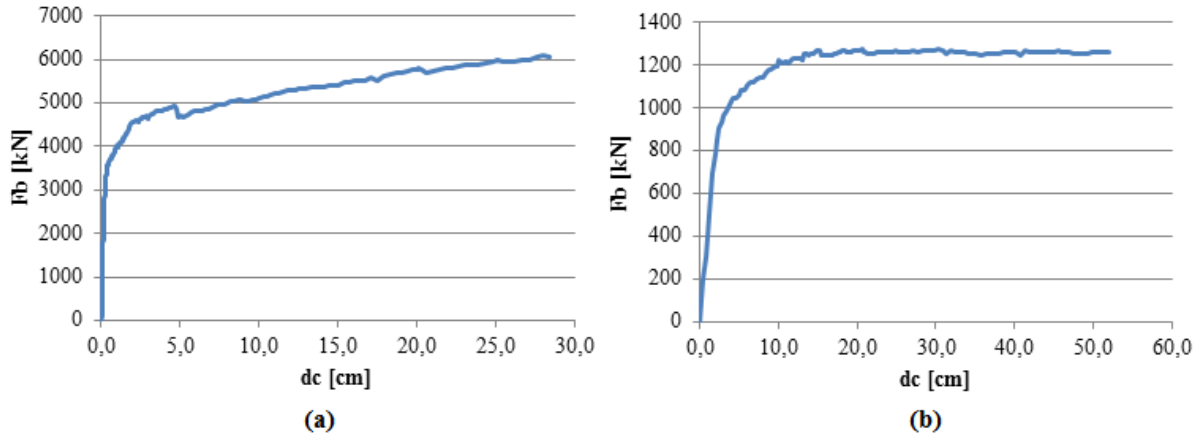

Figure 5: Capacity curves of the masonry structure for both in-plane (a) and out-of-plane (b) directions (third and first vibration mode respectively).

3 ROCKING BEHAVIOR OF THE PINNACLES

In this section, the dynamic behavior of the marble pinnacles regarded as rigid bodies is assessed. In particular, their rocking behavior under base excitations is analyzed, in order to assess their structural safety with regard to collapse by toppling.

3.1 Design seismic impulse at the base of the pinnacle

In the following analysis an impulsive seismic excitation acting on the pinnacle is considered. In order to obtain the design earthquake impulse, it is necessary to evaluate, at least in a conventional way, the amplification effect of the underlying masonry construction (a more sophisticated analysis for the evaluation of the amplification effect will be presented in Section 4).

As shown in Tab. 2, the fundamental period of the structure T_1 results equal to 0.49 s. As suggested in paragraph C8A.4.2.3 of [22], the design seismic acceleration acting on an object placed at a height Z on a construction may be evaluated with the approximated formula:

$$a_d = S_e(T_1) \cdot \Psi(Z) \cdot \gamma \tag{1}$$

where $S_e(T_1)$ is the design earthquake spectra evaluated in T_1, $\Psi(Z)$ is the first normalized vibration mode of the structure and γ is the corresponding participation factor. For an inverted triangular shape of the first mode, $\Psi(Z)$ can be evaluated with the formula $\Psi(Z) = Z/H$ where H is the maximum height of the construction.

For the case under study $S_e(T_1)$ is equal to 0.600 g. When considering central pinnacles, Z is equal to 18.25 m and $\Psi(Z)$ is equal to 1 whereas for lateral pinnacles Z is equal to 9.80 m and $\Psi(Z)$ is equal to 0.537. Finally, from the natural frequency analysis γ is equal to 1.2 for central pinnacles and equal to 1 for lateral pinnacles.

From equation (1) the design seismic acceleration a_d on central pinnacles results equal to 0.720 g whereas on lateral pinnacles of pinnacles is equal to 0.322 g.

3.2 Rocking motion of the pinnacles without isolation

In the present paper the rocking motion of the pinnacle is analyzed as a two-dimensional planar problem where the pinnacle is represented by one of its diametral sections [9], [10].

Let us assume that sliding between the pinnacle and its rigid base is prevented. In this case, in order to describe the two-dimensional rocking motion of the pinnacle under base excitations, a single Lagrangian parameter θ is needed. A possible choice for θ is the angle from the vertical as shown in Fig.6 where G indicates the center of mass of the rigid body which is lying on the symmetry axis, at a height z_G equal to 1.042 m above the base. Depending on the ground acceleration, the pinnacle may move rigidly with the ground or be set into rocking; in the letter case it will oscillate around the centers of rotation O and O'. Therefore, the problem is governed by two equation of motion. R represents the length of the segment connecting the center of mass G to one of the rotation centers.

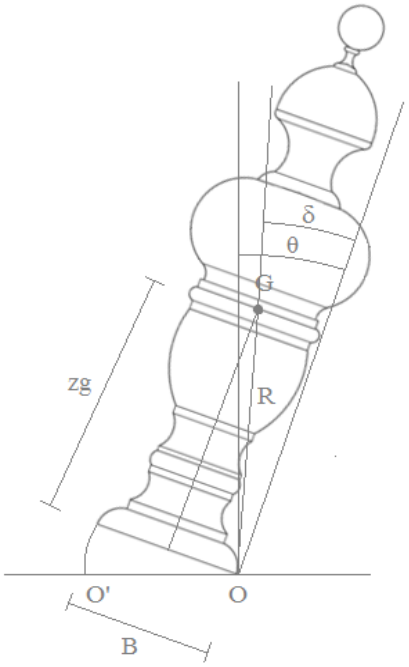

Figure 6: Rocking pinnacle.

When subjected to base acceleration $\bar{a}_g$ in the horizontal direction the pinnacle will be set into a rocking motion when the overturning moment of the horizontal inertia force about one of the centers of rotation exceeds the stabilizing moment due to the weight of the body:

$$\begin{aligned} M\,\bar{a}_g z_G &> M\,g\,\frac{B}{2} \\ \bar{a}_g &> \frac{B}{2z_g}\,g = 0.208g \end{aligned} \tag{2}$$

where M is the mass of the pinnacle and g is the acceleration of gravity. Equation (2) represents a necessary condition for the initiation of a rocking motion and is equivalent to a standard linear kinematic analysis as defined in [22]. For the present case-study, assuming $\bar{a}_g$ equal to the design seismic acceleration a_d calculated in Subsection 3.1, condition (2) is satisfied for both central and lateral pinnacles. Nevertheless, this condition does not guarantee the continuation of the rocking motion. In order to assess if, after initiation, a rocking motion of the pinnacles is established, it is necessary to look more in depth into the phenomenon.

The equations of motion of the pinnacle subjected to horizontal ground accelerations $a_g(t)$, governing the angle θ are derived by considering the equilibrium of moments about the centers of rotation. These equations can be expressed as

$$I_0\ddot{\theta} + MgR\sin(\delta-\theta) = -MR\cos(\delta-\theta)\,a_g(t) \tag{3}$$

when the pinnacle rocks about O and

$$I_0\ddot{\theta} - MgR\sin(\delta+\theta) = -MR\cos(\delta+\theta)\,a_g(t) \tag{4}$$

when it rocks about O'. In addition to the quantities defined earlier in Fig.6, I_0 represents the mass moment of inertia about O or O' and $\delta = \tan^{-1}\left(\mathrm{B}/2\,\mathrm{z}_G\right)$.

In particular for the present case study, $I_0 = 1434\,\mathrm{kg}\cdot\mathrm{m}^2$. Let us incidentally observe that the switching of equations back and forth between equations (3) and (4) during rocking motion, and the trigonometric functions of θ make equations (3) and (4) highly nonlinear.

At this point it is necessary to examine more closely the impact phase of the rocking motion. When the pinnacle is rotated through an angle θ and then released from rest with initial displacement, it will rotate about the center O and it will fall back into the vertical position. If the impact is assumed to be inelastic, the rotation continues smoothly about the center O' and the moment of the momentum about O' is conserved. Thus:

$$I_0\dot{\theta}_1 - MRB\dot{\theta}_1\sin\delta = I_0\dot{\theta}_2 \tag{5}$$

Dividing by $I_0\dot{\theta}_1$ Eqn. (5) gives the ratio between angular velocities after and before impact:

$$\frac{\dot{\theta}_2}{\dot{\theta}_1} = 1 - \frac{M}{I_0}RB\sin\delta. \tag{6}$$

If the ratio between angular velocities after and before impact is positive, then after impact the rotation of the pinnacle continues about the opposite center. If, conversely, angular velocity changes sign after impact the pinnacle bounces about the point of rotation prior to impact. Therefore, relationship (6) gives the following condition for the onset of a rocking motion:

$$\frac{MRB\sin\delta}{I_0} < 1 \tag{7}$$

which is satisfied for the pinnacle in our case study. Let us observe that condition (7) depends only on geometric and mass properties of the rigid body. This means that, whenever a rigid body, for which condition (7) holds, gets tilted by an initial angle (e.g. in case of an external seismic excitation satisfying condition (2) like in our case) then a rocking motion will be established. Conversely, if condition (7) does not hold, the block will bounce about the same corner and a proper rocking motion will not be established.

3.3 Overturning by single-pulse excitations

Dynamic behavior of rigid bodies under seismic actions is very complex and requires a time step integration of equations of motion in order to be fully described. Nevertheless, in order to assess the safety of pinnacles under dynamical conditions, useful information may be obtained from an analytical investigation of the collapse by overturning under single-pulse earthquake excitations.

In this subsection a simple overturning analysis for the pinnacles under single-pulse excitations is presented. The excitation may be a rectangular pulse with constant acceleration a_{g0} lasting for a time t_1 or acceleration varying as a half-cycle sine-wave pulse of amplitude a_{g0} and duration t_1. In the present case-study, as seen in the previous section, the motion of central pinnacles is initiated by the base acceleration $a_{g0} = a_d = 0.720\,\mathrm{g}$. Even if the motion is initiated (i.e. condition (2) satisfied) and the body is subjected to rocking motion (i.e. condition (7) satisfied) the body may or may not overturn depending on the magnitude of a_{g0} and the duration t_1. Housner [9] determined the duration t_1 of a rectangular pulse with acceleration a_{g0} required to overturn the block through the following equation:

$$\cosh\sqrt{\frac{MgR}{I_o}}t_1 = 1 + \left[1/\left(2\frac{a_{g0}}{g\delta}\left(\frac{a_{g0}}{g\delta} - 1\right)\right)\right]. \tag{8}$$

Analogously, for the half-cycle sine-wave pulse he derived the following equation relating the duration t_1 to the amplitude a_{g0} of the excitation:

$$\frac{a_{g0}}{g\delta} = \sqrt{\left[1 + \frac{I_0}{MgR}\left(\frac{\pi}{t_1}\right)^2\right]} \tag{9}$$

This equations were determined in [9] starting from the linearized version of equations (3) and (4); therefore, they are valid only for slender blocks (like the ones in our case-study).

Let us study the case of central pinnacles. Considering the geometrical and mass properties of the pinnacles and assuming $a_{g0} = a_d = 0.720\,\mathrm{g}$ equation (8) gives an overturning duration for the rectangular pulse excitation of $t_1 = 0.15\,\mathrm{s}$, while equation (9) gives an overturning duration for the sine-wave pulse excitation of $t_1 = 0.48\,\mathrm{s}$.

As shown in [24] typical pulse duration for earthquakes of low to medium intensity is between 0.10 s and 0.50 s. This means that the pulse-type excitations considered in this Section, with the computed duration t_1 that brings to collapse the pinnacles by overturning, are typical

of earthquakes that may occur in the Ferrara area. This corroborates the conclusion that pinnacles in our case-study are not safe under design seismic actions.
For these reasons, a base isolation system has been designed in order to protect pinnacles from potential earthquake excitations.

4 THE ISOLATION SYSTEM

This section contains a description of the base isolation system, which has been specifically devised for the protection of the pinnacles of the Ferrara city-gate.

4.1 The isolation system

Both lateral and central pinnacles are isolated through the use of double concave curved surface steel sliders. A schematic representation of the single isolator is depicted in Fig.7a. Two different isolating systems have been devised respectively for central pinnacles and lateral pinnacles.

For the three central pinnacles the isolating system for each pinnacle is made of three isolators placed at the vertex of a equilateral triangle and rigidly connected together by an upper steel plate on which the pinnacle lies. The system is schematically depicted in Fig.8a.

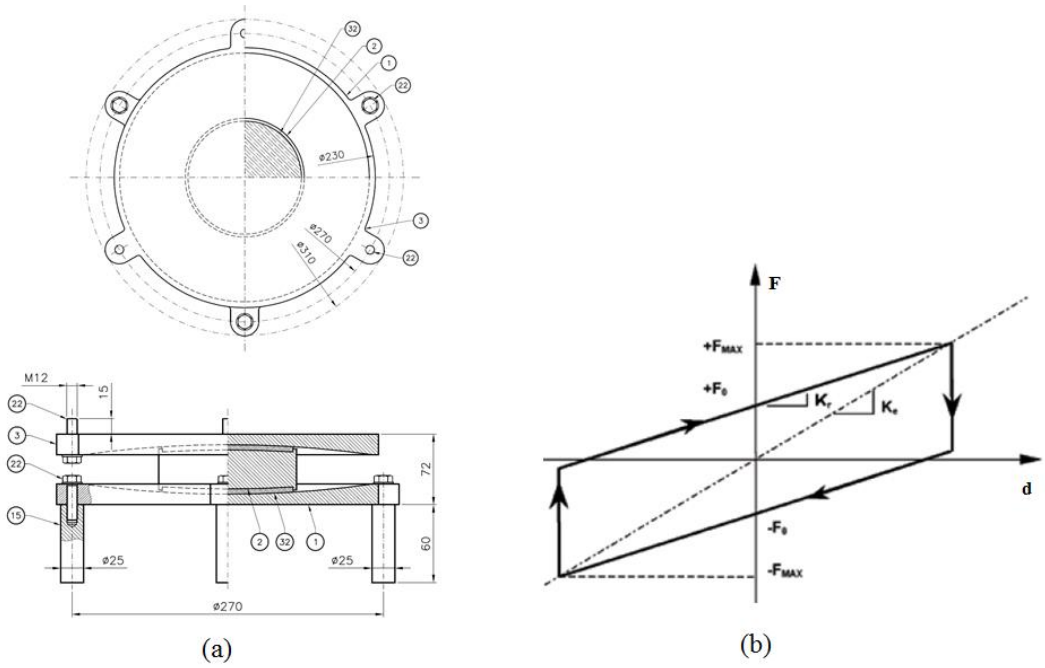

Figure 7: (a) Schematic view of the seismic isolator: a double concave curved surface steel slider developed and produced by the Research and Development Department of FIP Industriale Group; (b) force-displacement response of the isolator.

For each of the two groups of four lateral pinnacles the isolating system is made of four isolators (one beneath each pinnacle) connected together by a system of steel rods and plates which guarantees an approximatively zero relative displacement between isolators. In fact, the system may be regarded as a wide isolated base on which the four pinnacles lie. The system is schematically depicted in Fig.8b.

Thus, for the isolation of all the eleven pinnacles seventeen isolators will be employed.

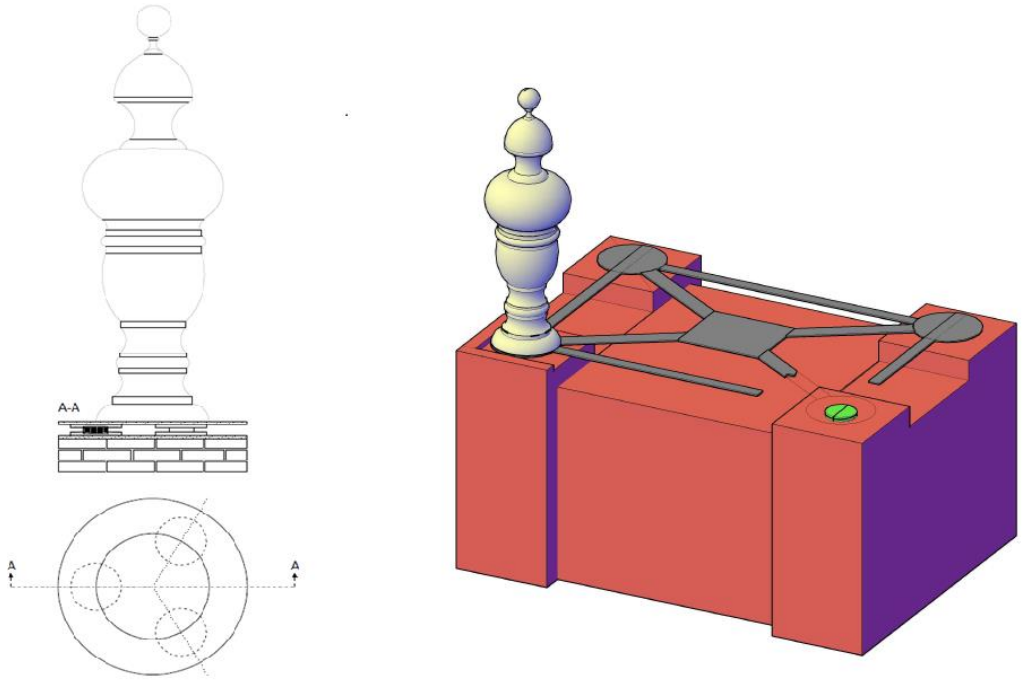

Figure 8: Isolating system devised for central pinnacles (a), and lateral pinnacles (b).

4.2 Mechanical properties of the steel sliders

According to producer specifications isolators force-displacement response is represented by a rigid-plastic with hardening and friction like behavior of the kind depicted in Fig.7b where F_0 is the maximum friction force which the isolator can develop, K_r is the stiffness of the hardening-like branch, $F_{\max}$ is the maximum force can develop at the end of the hardening-like branch. These quantities are defined by the following relations [19], [25]:

$$\begin{cases} F_0 = \mu N_{Sd}\,; \\ K_r = \dfrac{N_{Sd}}{R}\,; \\ F_{\max} = F_0 + K_r d\,; \end{cases} \tag{10}$$

where μ is the friction coefficient along the sliding surface, N_{Sd} is the vertical load acting upon the isolator, R is the equivalent curvature radius of the sliding surface and d is the maximum allowed displacement. Furthermore, an equivalent damping coefficient ξ_e can be defined through the following formula

$$\xi_e = \frac{2}{\pi}\left(\frac{d}{\mu R}+1\right)^{-1}. \tag{11}$$

Friction coefficient μ is a function of the vertical load N_{Sd} and temperature. Therefore, the producer has not provided this value for the isolators used, but a range of values varying between 0.5% and 2.5%. In the following analysis both these two values of μ have been taken into consideration.

Tab.3 summarize the mechanical properties for isolators used in the two isolation systems for the two different values of the friction coefficient.

	N_{Sd}	d	R	ξ_e	F_0	K_r	F_{max}
	[kN]	[mm]	[mm]	[-]	[kN]	[N/mm]	[kN]
$\mu = 2.5\%$	3.33	150	2000	0.16	0.083	1.665	0.333
$\mu = 0.5\%$	3.33	150	2000	0.04	0.016	1.665	0.266

Table 3 Mechanical properties of the steel sliders isolation devices used.

5 NUMERICAL SIMULATIONS

In order to assess the effectiveness of the isolation system in preventing rocking and overturning of the pinnacles, time-history dynamic analyses with a seismic accelerogram applied to the base of the isolated pinnacle have been carried out and are described in this Section.

5.1 Design accelerograms and amplification effect

In order to evaluate the dynamic response of the pinnacle, the definition of a design accelerogram is necessary.

As required by Italian Building Code [20] and Eurocode 8 [26], a set of seven accelerograms compatible with the earthquake design spectrum of the site, defined in [20] for a ultimate limit state in terms of collapse, has been generated with the software Rexel 3.5.

For each accelerogram the corresponding spectrum (reported in Fig.9) can be generated.

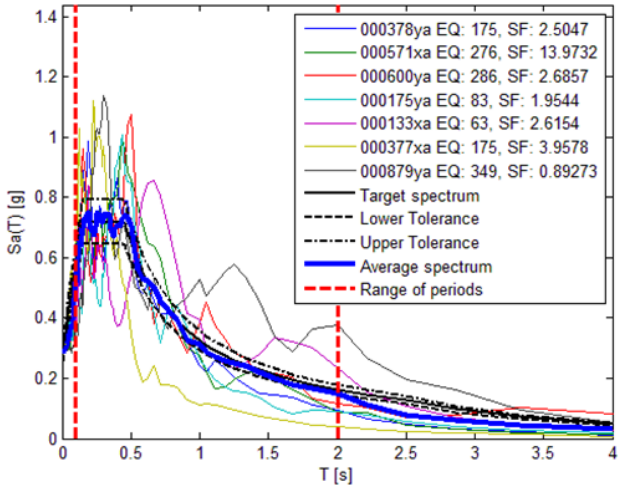

Figure 9: Earthquake spectra compatible with the design spectra defined by NTC2008 generated with Rexel 3.5.

In order to define the correct seismic action on the pinnacles, it is necessary to take into account the amplification effect due to the underlying masonry structure. Thus, for each spectrum compatible accelerogram, applied at the base of the structure as a forcing action, two different time-history dynamic analyses of the three-arched masonry city gate have been carried out using the finite element analysis software Straus7, one with the ground accelerations applied in the in-plane direction and one with the ground accelerations applied in the out-of-plane direction. Therefore, a total of fourteen analyses have been conducted.

The finite element model used is the same described in paragraph 2.3. Masonry has been modeled as a linear visco-elastic material with a Raleigh damping model. Rayleigh damping,

also known as proportional damping, assumes that the global damping matrix $\mathbf{C}$ is a linear combination of the global stiffness $\mathbf{K}$ and mass $\mathbf{M}$ matrices:

$$\mathbf{C} = \alpha\mathbf{M} + \beta\mathbf{K} \qquad (12)$$

where α and β are constants of proportionality. The two constants α and β are normally determined by using the following relationship

$$\xi = \frac{1}{2}\left(\frac{\alpha}{\beta} + \beta\omega\right) \qquad (13)$$

for two values of the damping ratio ξ_1 and ξ_2 at two chosen frequencies ω_1 and ω_2. Substituting the two sets of ξ and ω values into (13) the following two equations for α and β are obtained:

$$\alpha = \frac{2\omega_1\omega_2\left(\xi_2\omega_1 - \xi_1\omega_2\right)}{\omega_1^2 - \omega_2^2};\ \beta = \frac{2\left(\xi_1\omega_1 - \xi_2\omega_2\right)}{\omega_1^2 - \omega_2^2}. \qquad (14)$$

In the non-linear dynamic finite element analysis related to our case-study the values of α and β for the Raleigh damping model where determined through equation (14) assuming for ω_1 and ω_2 the frequencies of the two principal modes (respectively the out-of-plane and in-plane translational modes which were obtained through the natural frequency analysis) and for ξ_1 and ξ_2 the values 10% and 5% respectively as suggested in [27]. The choice of such equivalent viscous damping coefficient is justified in the subsequent paragraph through an ad-hoc numerical procedure.

At the end of each time-history dynamic analysis the response of the structure in terms of acceleration at the base of both lateral and central pinnacles have been recorded. This response represents the design seismic accelerogram to be applied at base of the isolated pinnacles in order to assess the effectiveness of the isolation system.

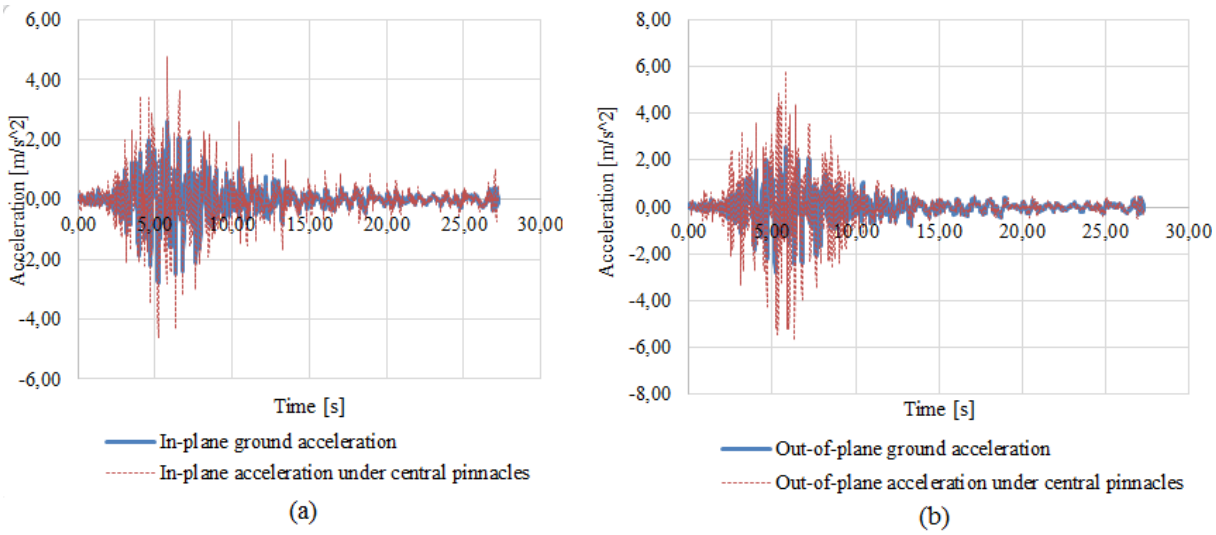

Figure 10: Amplification of the base seismic action 378ya due to the masonry structure on central pinnacles in the in-plane (a) and out-of-plane (b) directions.

Fig.10a-b depict a comparison between the accelerogram 378ya applied at the ground level in the two main directions respectively and the corresponding accelerogram computed at the

level of central pinnacles. Analogous results are obtained for lateral pinnacles and are here omitted for the sake of brevity.

5.2 Numerical evaluation of masonry equivalent viscous damping coefficients ξ_1 and ξ_2

In this paragraph the numerical procedure used to estimate the equivalent viscous damping coefficients ξ_1 and ξ_2 for masonry is outlined. The procedure is similar to the one described in [28] and is aimed to obtain a consistent value of the viscous damping coefficients that can be used within standard finite-element time-history dynamic analyses with the Rayleigh damping model described in the previous paragraph. More precisely, the equivalent viscous damping coefficient is assumed varying with the maximum displacement level reached by the structure during earthquake solicitation. Thus, the goal is to determine the relation between the equivalent viscous damping coefficient and the maximum displacement that the structure can reach under seismic actions. The algorithm, for each loading direction (in- and out-of-plane), can be summarized in the following steps:

1. A capacity curve of the masonry structure in a given loading direction is computed as explained in paragraph 2.3. This curve allows to determine the maximum displacement which the structure may undergo before collapse occurs.
2. The capacity curve obtained in Step 1 is reduced to the capacity curve of an equivalent single degree-of-freedom (d.o.f.) system following prescriptions contained in §C7.3.4.1 of [22]. Then, the new single d.o.f. capacity curve is further simplified to a bi- or tri-linear curve.
3. A hysteretic force-displacement law is assigned to the equivalent single d.o.f. structure which allows to evaluate the response of the structure under cyclic loading. In what follows, two hysteretic models will be used: a classical elastic-perfectly plastic law, which has the bi-linear curve determined in Step 2 as skeleton curve, and a newer inelastic model similar to the one described in [28] which uses the tri-linear curve determined in Step 2 as skeleton curve.
4. Since the aim is to determine a curve which relates the maximum displacement reached by the structure during seismic action and the equivalent viscous damping coefficient, it is necessary to fix several reference displacement values which subdivide the nonlinear part of the fixed skeleton curve. Furthermore, for each reference displacement value, the secant stiffness on the skeleton curve can be computed and stored.
5. For each reference displacement value nonlinear time-history dynamic analyses on the equivalent single d.o.f. structure with the chosen hysteresis constitutive model is carried out. Each analysis is performed with an external base acceleration history obtained from each of the seven spectrum-compatible accelerograms defined in paragraph 5.1 multiplied by a multiplication factor chosen so that the maximum displacement reached during the analysis is equal to the considered reference displacement value. The corresponding multiplication factor is saved as the value which gives the accelerogram which, acting on the structure, produces a maximum displacement equal to the reference displacement value considered.
6. A reference displacement value is fixed. A linear elastic single d.o.f. system equivalent to the non-linear single d.o.f. system is defined by assigning the secant stiffness computed in Step 4 for the assigned reference displacement value and an equivalent viscous coefficient determined though an iterative procedure: given the reference displacement value, a trial equivalent viscous coefficient is assigned to the system and a linear time-history analysis under the action of the design accelerogram multiplied by

the factor corresponding to the reference displacement value determined in Step 5 is carried out. The maximum displacement obtained through the linear time-history analysis is compared with the expected maximum displacement from the non-linear time-history analysis carried in Step 5. Then, the trial equivalent viscous coefficient is suitably changed and the linear analysis performed again until the maximum displacements obtained from linear and non-linear time-history analyses coincide. The corresponding value of the equivalent viscous damping coefficient is the value which corresponds to the assigned displacement reference value.

By going through Step 6 for each reference displacement value it is possible to obtain the curve relating the equivalent viscous damping coefficient to the corresponding value of the maximum displacement the structure undergoes. The described algorithm has been implemented within a MATLAB script and single d.o.f. time history dynamic analyses have been carried out using a Newmark type integration algorithm.

5.2.1 Out-of-plane equivalent viscous damping coefficient ξ_1

Both bilinear and trilinear approximations of the single d.o.f. out-of-plane capacity curve for the masonry structure, depicted in Fig. 11, are considered and ten reference displacement values are marked on each curve.

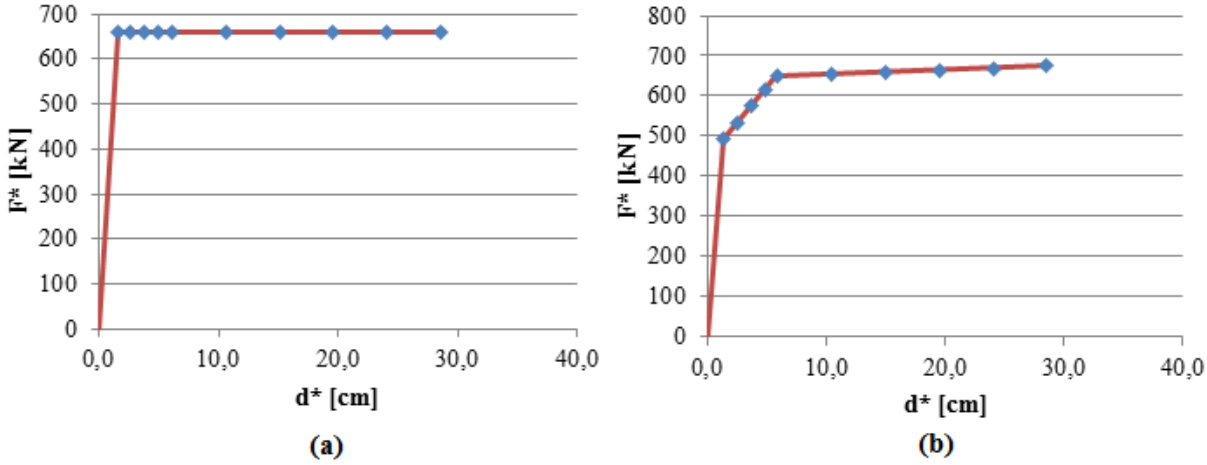

Figure 11: Bilinear (a) and trilinear (b) approximations of the single d.o.f. out-of-plane capacity curve for the masonry structure. Solid squares indicate reference displacements values.

The procedure described in the previous paragraph has been carried out for each of the seven spectrum compatible design accelerograms and for both the bilinear elastic-perfectly plastic and the trilinear Nicolini-type constitutive laws. In Fig. 12 a comparison between the single d.o.f. non-linear time-history analysis with both bilinear and trilinear inelastic laws and the final linear time-history analysis in Step 6 for a reference displacement equal to respectively 5.0 and 5.9 cm is shown for one of the seven spectrum-compatible accelerograms.

Fig. 13 depicts the final relation obtained at the end of the procedure, for each assigned reference displacement value, between equivalent viscous damping coefficient and the maximum out-of-plane displacement value the structure undergoes when it is subjected to seismic actions. In particular, the portrayed diagram is the average result obtained by repeating the numerical procedure described for each of the seven spectrum-compatible accelerograms.

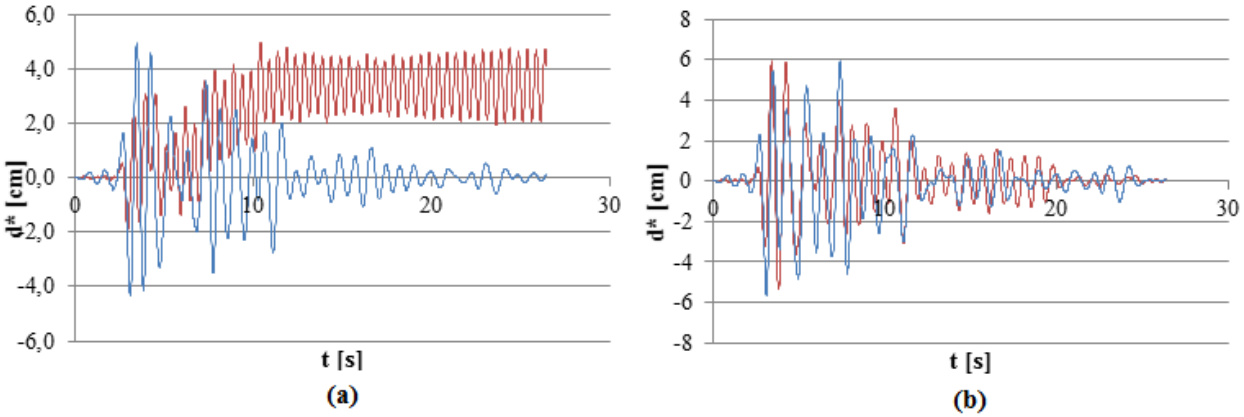

Figure 12: Comparison between inelastic time history analysis (red) and equivalent linear time history analysis (blue) for bilinear constitutive law and reference displacement value d = 5.0 cm (a) and trilinear constitutive law and reference displacement value d = 5.9 cm (b). Analyses conducted for accelerogram 378ya.

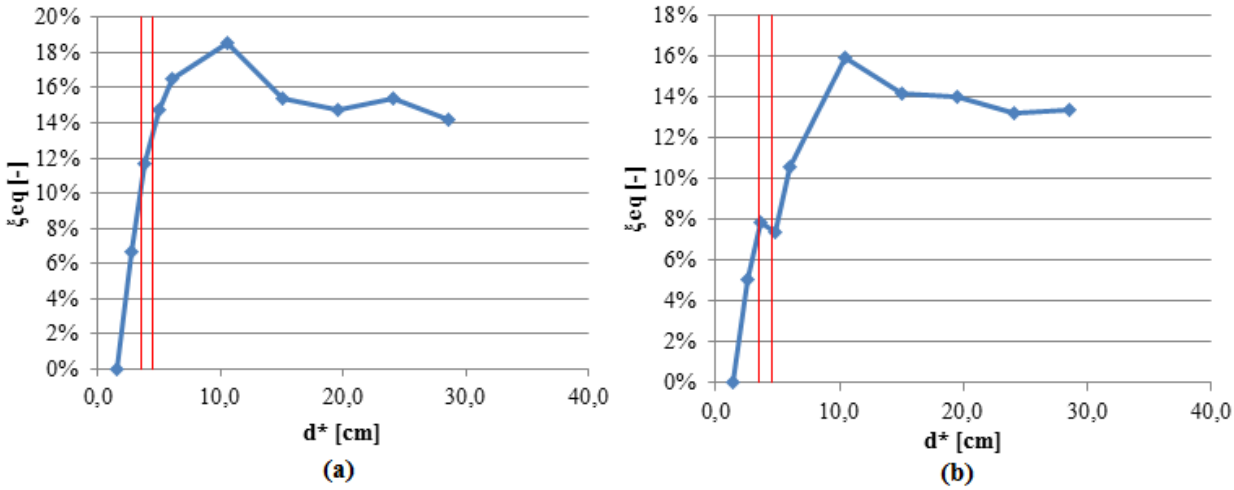

Figure 13: Final relation between equivalent viscous damping coefficient and the maximum out-of-plane displacement the structures may undergo for both bilinear constitutive law (a) trilinear constitutive law (b).

From an out-of-plane pushover analysis carried out according to [20] it is possible to infer that for the design earthquake, the maximum displacement the structure undergoes is 4.1cm. It is therefore reasonable to assume, for the evaluation of the equivalent viscous damping coefficient to be used in subsequent analyses, a displacement range of 3.5-4.5cm. In this range equivalent viscous damping coefficient varies between 10.25% and 13.52% when considering the bilinear constitutive law and of 7.5% when considering the trilinear constitutive law. It is then justified the use of the value $\xi_1 = 10\%$ as largely suggested in literature for masonry constructions (see, e.g. [27]).

5.2.1 In-plane equivalent viscous damping coefficient ξ_2

In analogy with the case discussed in the previous paragraph, both bilinear and trilinear approximations of the single d.o.f. in-of-plane capacity curve for the masonry structure, depicted in Fig. 14, are considered and ten reference displacement values are fixed on each curve.

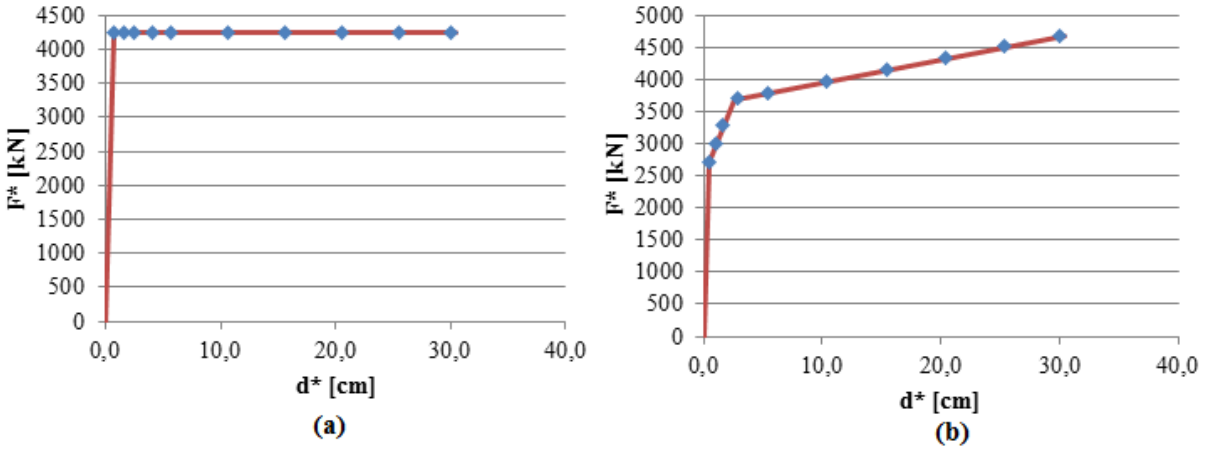

Figure 14: Bilinear (a) and trilinear (b) approximations of the single d.o.f. in-plane capacity curve for the masonry structure. Solid squares indicate reference displacements values.

Again, in Fig. 15 a comparison between the single d.o.f. in-plane non-linear time-history analysis with both bilinear and trilinear inelastic laws and the final linear time history analysis in Step 6 for a reference displacement equal to respectively 5.7 and 5.4 cm is shown for one of the seven spectrum-compatible accelerograms.

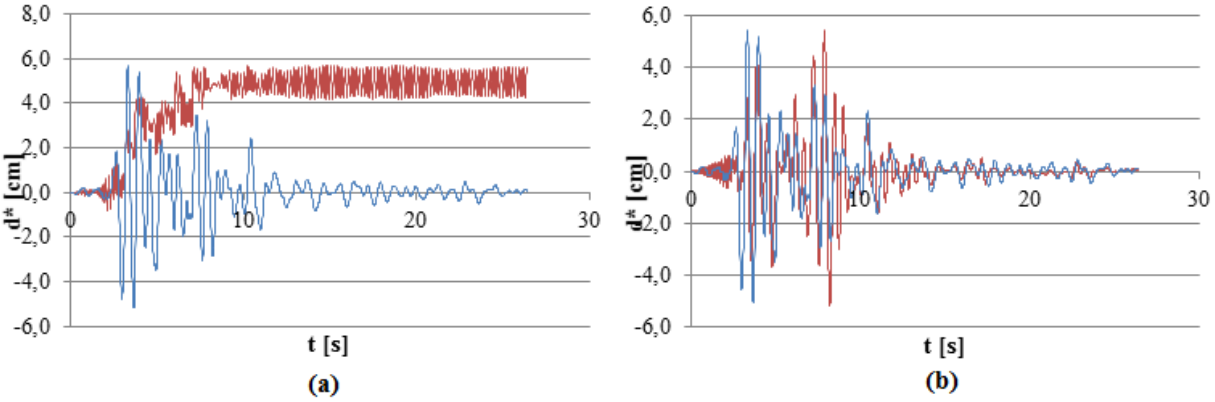

Figure 15: Comparison between inelastic time history analysis (red) and equivalent linear time history analyses (blue) for bilinear constitutive law and reference displacement value d = 5.7 cm (a) and trilinear constitutive law and reference displacement value d = 5.4 cm (b). Analysis conducted for accelerogram 378ya.

Fig. 16 depicts the final relation obtained at the end of the procedure, for each assigned reference displacement value, between equivalent viscous damping coefficient and the maximum in-plane displacement value the structure undergoes when it is subjected to seismic actions. In particular, the portrayed diagram, is the average result obtained by repeating the numerical procedure described for each of the seven spectrum-compatible accelerograms.

From an in-plane pushover analysis carried out according to [20] it is possible to infer that for the design earthquake, the maximum displacement the structure undergoes is 1.1cm. It is therefore reasonable to assume, for the evaluation of the equivalent viscous damping coefficient to be used in subsequent analyses, a displacement range of 0.5-1.5cm. In this range equivalent viscous damping coefficient varies between 0.0% and 8.0% when considering the bilinear constitutive law and between 1.35% and 12.70% when considering the trilinear constitutive law.

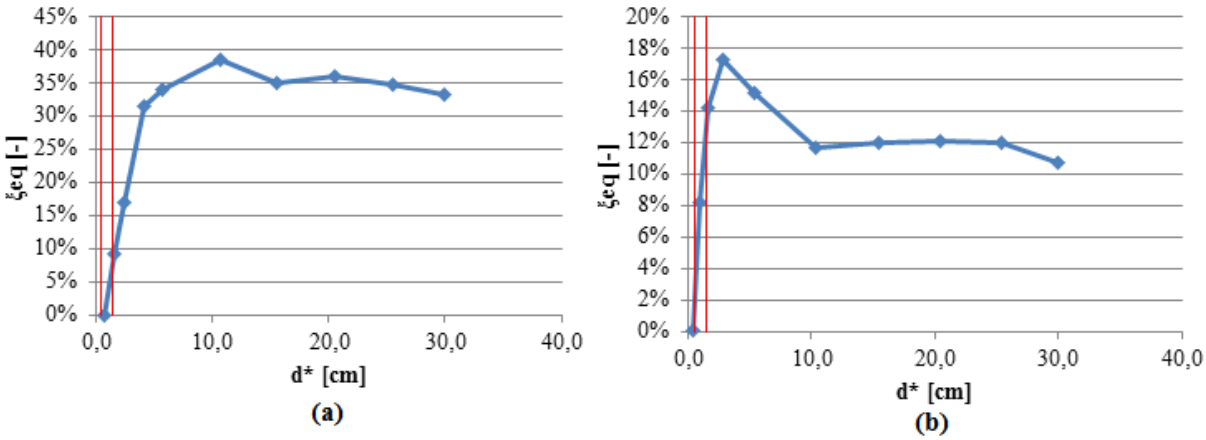

Figure 16: Final relation between equivalent viscous damping coefficient and the maximum in-plane displacement the structures may undergo for both bilinear constitutive law (a) trilinear constitutive law (b).

The value of $\xi_2 = 5\%$ largely suggested in literature for masonry constructions (see, e.g. [27]) is well within these ranges and thus, its use in the subsequent analyses is justified.

5.3 Non-linear dynamic analysis of the isolated pinnacles

In order to establish the seismic response of the isolated pinnacles and the effectiveness of the isolation system, time-history non-linear dynamic analyses with the amplified base accelerograms previously determined, have been conducted using the finite element software Straus7. Isolation system has been modeled as a parallel system of a spring and a damper, whereas the pinnacle has been modeled as a non-structural mass. Spring stiffness and damping coefficient for the damper are respectively K_r and ξ_e as defined in Tab. 3, considering both friction coefficients of 2.5% and 0.5%.

Results in terms of acceleration response to the amplified ground accelerogram 378ya for central pinnacles in both in-plane and out-of-plane directions are reported in Fig.17a-b respectively, for both friction coefficients, whereas results in terms of displacement response to the amplified ground accelerogram 378ya for central pinnacles are reported in Fig.17c-d respectively, for both friction coefficients.

As can be observed, the maximum acceleration transferred to the pinnacles is, in every case, smaller than the minimum value required to initiate rocking motion defined by equation (2).

Finally, it is to be noticed that the maximum displacement which the pinnacle undergoes is, in every case, smaller than the maximum displacement allowed by the isolators, which is equal to 0.15 m (see Tab.3).

Results in terms of acceleration response to the amplified ground accelerogram 378ya for lateral pinnacles in both in-plane and out-of-plane directions are analogous and for the sake of brevity are not reported in the following. Therefore, the effectiveness of the isolation system devised for the protection of the marble pinnacles from seismic excitations has been assessed for each pinnacle.

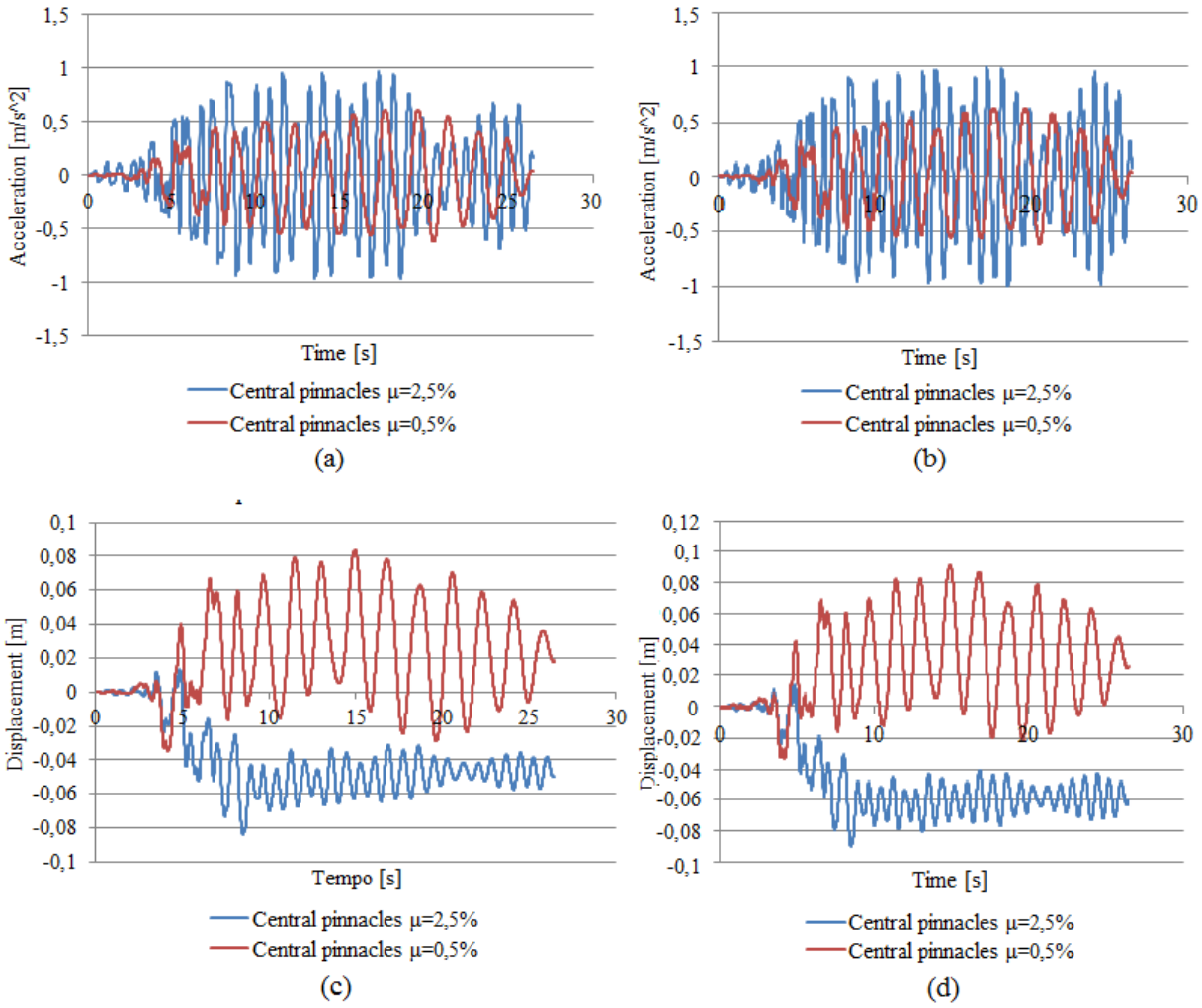

Figure 17: Response of central pinnacles to the seismic action defined by (amplified) accelerogram 378ya in terms of in-plane (a) and out-of-plane (b) acceleration, in-plane (c) and out-of-plane (d) displacements.

6 CONCLUSIONS

This contribution addressed the problem of seismic protection of heavy non-structural objects placed at the top of monumental masonry constructions through the illustration of the case study of the eleven marble monolithic pinnacles placed at the top of the three-arched masonry city gate in Ferrara.

The underlying masonry structure has been characterized with a natural frequency finite element analysis and through the computation of capacity curves with finite-element non-linear incremental analyses. Rocking motion and the safety against toppling of the pinnacles, regarded as rigid bodies under pulse-type earthquake excitations, have been discussed, showing that they are not safe under the design seismic action as defined by [20].

A seismic isolation system for the prevention of rocking and overturning phenomena has been devised and its effectiveness has been established through non-linear time-history dynamic analyses of the pinnacles under earthquake action expressed through base accelerograms, which are spectrum compatible with the design seismic action.

The amplification effect on the ground accelerations due to the underlying structure has been taken into account through time history dynamic analyses in which a Rayleigh damping model was adopted. A procedure for the estimation of the equivalent viscous damping coeffi-

cient for masonry has been outlined and the obtained values have been proven to be in agreement with the ones suggested in literature.

Non-linear time history dynamic analyses showed that the isolation system is effective in reducing seismic action transmitted to the pinnacles through the main structure, enough to prevent any rocking motion or overturning phenomena.

REFERENCES

[1] G.L. McGavin, *Earthquake protection of essential building equipment*, John Wiley and Sons, 1981.

[2] M.S. Agbabian, S.F. Masri, R.L. Nigbor, W.S. Ginell, Seismic damage mitigation concepts for art objects in museums, In: *Proceedings of 9th world conference on earthquake engineering*, Tokyo-Kyoto, Japan, August 1988.

[3] G. Augusti, M. Ciampoli, Guidelines for protection of museum contents, In: *Proceedings of 11th world conference on earthquake engineering*, Acapulco, Mexico, June 1996.

[4] F. Vestroni, S. Di Cintio, Base isolation for seismic protection of statues, In: *Proceedings of 12th world conference on earthquake engineering*, Auckland, New Zealand, June 2000.

[5] P.C. Roussis, E.A. Pavlou, E.C. Pisiara, Base-isolation technology for earthquake protection of art objects, In: *Proceedings of 14th world conference on earthquake engineering*, Beijing, China, October 2008.

[6] I. Caliò, M. Marletta, Passive control of the seismic rocking response of art objects, *Engineering Structures*, Vol. 25, 2003, pp. 1009-1018.

[7] A. Contento, A. Di Egidio, Seismic protection of monolithic objects of art using a constrained oscillating base, In. *Advances in Geotechnical Earthquake Engineering - Soil Liquefaction and Seismic Safety of Dams and Monuments*, Edited by Abbas Moustafa, InTech, 2012.

[8] H. Kimura, K. Iida, On rocking of rectangular columns, *Journal of the Seismological Society of Japan*, Vol 6., No. 3, 1934, pp. 125-149.

[9] G.W. Housner, The behavior of inverted pendulum structures during earthquakes, *Bulletin of the Seismological Society of America*, Vol. 53, No. 2, 1963, pp. 403-417.

[10] W.K. Yim, A.K. Chopra, J. Penzien, Rocking response of rigid blocks to earthquakes, *Earthquake Engineering and Structural Dynamics*, Vol. 8, No. 6, 1980, pp. 565-587.

[11] A. Di Egidio, A. Contento, Base isolation of sliding-rocking non-symmetric rigid blocks subjected to impulsive and seismic excitations, *Engineering Structures*, Vol. 31, 2009, pp. 2723-2734.

[12] A. Di Egidio, A. Contento, Seismic response of a non-symmetric rigid block on a constrained oscillating base, *Engineering Structures*, Vol. 32, 2010, pp. 3028-3039.

[13] M.F. Vassiliou, N. Makris, Analysis of the rocking response of rigid blocks standing free on a seismically isolated base, *Engineering Structures*, Vol. 41, No. 2, 2011, pp. 177-196.

[14] A.S. Koh, G. Mustafa, Free rocking of cylindrical structures, *Journal of Engineering Mechanics*, Vol. 116, 1990, pp. 34-54.

[15] A. Magravanis, I. Stefanou, I. Vardoulakis, Dynamic motion of a conical frustum over a rough horizontal surface, International Journal of Non-Linear Dynamics, Vol. 46, No. 1, 2011, pp. 114-124.

[16] Y. Li, B. Shi, Response of 3D free axisymmetric rigid objects under seismic excitations, *New Journal of Physics*, 2010.

[17] M. Lowry, D. Armendariz, B.J. Farra, J. Podany, Seismic mount making: a review of protection of objects in the J. Paul Getty museum from earthquake damage, In: *Advances in the protection of museum collections from earthquake damage*, symposium held at the J. Paul Getty museum at the Villa on May 3-4, 2006.

[18] L. Berto, T. Favaretto, A. Saetta, Seismic risk mitigation technique for art objects: experimental evaluation and numerical modelling of double concave curved surface sliders, *Bulletin of Earthquake Engineering*, Vol. 11, 2013, pp. 1817-1840.

[19] L. Berto, T. Favaretto, A. Saetta, F. Antonelli, F. Lazzarini, Assessment of seismic vulnerability of art objects: the "Galleria dei prigioni" sculptures at the Accademia Gallery in Florence, *Journal of Cultural Heritage*, Vol. 13, No. 1, 2012, pp. 7-21.

[20] NTC2008, Norme Tecniche per le Costruzioni, D.M. 14/01/2008, S.O. n. 30 G.U. n. 29, 4/2/2008.

[21] HSH, "Straus7, Finite Element Analysis System", hsh.info, 2014.

[22] CIRC2009, Circolare sulle "Nuove Norme tecniche per le costruzioni" di cui al DM 14/01/2008, S.O. n. 27, G.U. n. 47, 26/02/2009.

[23] TNO-DIANA, "DIANA, Finite Element Analysis", www.tnodiana.com, 2015

[24] V. Gioncu, F. Mazzolani, *Earthquake engineering for structural design*, CRC Press, 2010.

[25] J.M. Kelly, *Earthquake resistant design with rubber*, Springer-Verlag, 1993.

[26] EN1998, "Eurocode 8: Design of structures for earthquake resistance", 2004.

[27] F. Peña, P.B. Lourenço, N. Mendes, D. Oliveira, Numerical models for the seismic assessment of an old masonry tower, *Engineering Structures*, Vol. 32, 2010, pp. 1466-1478.

[28] Nicolini L., 2012. Equivalent viscous damping and inelastic displacement for strengthened and reinforced masonry walls. Ph. D. Thesis, University of Trento.